01 Jan 1975

The Application Of Impact Dampers To Continuous Systems

Ranjit K. Roy

Richard D. Rocke
Missouri University of Science and Technology

J. Earl Foster
Missouri University of Science and Technology

Recommended Citation

R. K. Roy et al., "The Application Of Impact Dampers To Continuous Systems," *Journal of Manufacturing Science and Engineering, Transactions of the ASME*, vol. 97, no. 4, pp. 1317 - 1324, American Society of Mechanical Engineers, Jan 1975.
The definitive version is available at https://doi.org/10.1115/1.3438755

Ranjit K. Roy
Senior Design Engineer,
Burroughs Corp.,
Detroit, Mich.

Richard D. Rocke
Senior Staff Engineer,
Hughes Aircraft Company,
Fullerton, Calif.

J. Earl Foster
Professor,
Engineering Mechanics Department,
University of Missouri-Rolla,
Rolla, Mo.

The Application of Impact Dampers to Continuous Systems

A study has been made of the application of impact dampers to two types of continuous systems, a simply supported and a clamped beam. Experimental models were tested in the laboratory and computer programs were developed to calculate response by two separate approaches. Results from calculations agreed favorably with experimental tests. Curves presented show the response to be expected for values of significant system parameters and enable the user to apply impact dampers to these types of continuous systems.

Introduction

An impact damper consists of a mass particle constrained to move between the two ends of a rigid container. When attached to a vibrating mechanical system the collision of the particle with the container boundaries results in a reduction of the vibration amplitude of the primary system through momentum transfer. An impact damper attached to a single degree-of-freedom system is shown in Fig. 1.

Grubin [1],[1] Arnold [2], and Masri and Caughey [3] have investigated the motion of the system shown in the figure. Masri [4] has also investigated the response of multi-degree-of-freedom systems with an impact damper and presented the exact solution for the steady state motion of the system. Recently Masri [5, 6] has extended his investigation to cover a class of uniform Bernoulli-Euler beams and plates of arbitrary shape.

The objective of the present study is to investigate the motion of a *continuous* system under the action of an impact damper. Two types of uniform, continuous beams subjected to sinusoidal base excitation are considered for analysis. Solutions valid between the impacts were obtained analytically by two separate approaches. In the first approach the mass of the damper container attached to the beam is assumed to be negligible and the solution is obtained for a viscously damped, Bernoulli-Euler beam. The solution satisfying the initial conditions is determined in terms of the sum of an infinite series.

In the second method, the uniform, continuous beam is replaced by a multi-degree-of-freedom discrete structure and the set of governing differential equations is solved exactly. The solution satisfies the initial conditions and defines the motion of the system from collision to collision.

It proved advantageous to use the discrete mass model in the current problem and the solution for the Bernoulli-Euler beam was used to verify the former approach. With the discrete model, for example, the mass of the damper container was incorporated and although not included in this paper, more complicated structural members could be studied.

Experiments were conducted with models of the two types of beams and damper units of three different weights with adjustable clearance. Base excitations used in various cases were different. These investigations produced system damping and the results were compared with analytical solutions.

1 Continuous System Solution

For the conventional, continuous beam system shown in Fig. 2, two types of damping were assumed. Internal damping was included in the constitutive equation as

$$\sigma = E\epsilon + C_{\text{int}}\frac{\partial \epsilon}{\partial t} \tag{1}$$

while external damping was assumed proportional to the relative beam velocity.

Based on equation (1), the bending moment has a second term

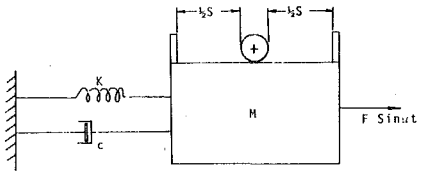

Fig. 1 Single-degree-of-freedom system with an attached impact damper

[1] Numbers in brackets designate References at end of paper.

Contributed by the Design Engineering Division and presented at the Design Engineering Technical Conference, Washington, D.C., September 17–19, 1975, of THE AMERICAN SOCIETY OF MECHANICAL ENGINEERS. Manuscript received at ASME Headquarters June 4, 1975. Paper No. 75-DET-81.

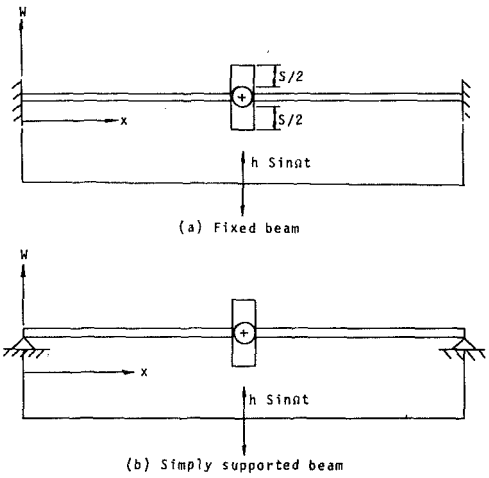

Fig. 2 A sketch of the continuous systems discussed in this report

due to the internal damping. The equation is

$$M(x) = EI\frac{\partial^2 W}{\partial x^2} + IC_{\text{int}}\frac{\partial^3 W}{\partial x^2 \partial t}. \quad (2)$$

From elementary considerations

$$\frac{\partial^2 M}{\partial x^2} = p(x,t) - \frac{\partial^2 W}{\partial t^2} - C_{\text{ext}}\frac{\partial W_r}{\partial t}. \quad (3)$$

Combining equation (2) and equation (3) gives the differential equation of motion

$$EI\frac{\partial^4 W}{\partial x^4} + IC_{\text{int}}\frac{\partial^5 W}{\partial x^4 \partial t} + \rho a\frac{\partial^2 W}{\partial t^2} + C_{\text{ext}}\frac{\partial W_r}{\partial t} = p(x,t).$$

The beams treated herein are displacement excited with harmonic motion and the loading function, $p(x,t)$, is taken to be zero. The absolute and relative beam displacements are related through

$$W(x,t) = W_r(x,t) + h\sin\Omega t.$$

Boundary conditions are

$$W(0,t) = W(L,t) = h\sin\Omega t.$$

As indicated in Fig. 2, two cases are considered in the paper, a beam clamped and another simply supported. For both, an impact damper was installed in the mid-position.

The solution for each case can be expressed in terms of beam functions as

$$W(x,t) = \sum_{n=1}^{\infty}\{\exp(-\beta_n t)(A_n\cos(\omega_{dn}t) + B_n\sin(\omega_{dn}t)) + F_n\sin(\Omega t - \Psi_n)\}U_n(x) + h\sin\Omega t \quad (4)$$

where

$$F_n = \frac{H_n h\Omega^2}{C_1\sqrt{(\omega_n^2 - \Omega^2)^2 + (2\beta_n\Omega)^2}},\quad 2\omega_n\xi_n = \frac{C_{\text{ext}}}{\rho a} + \frac{\omega_n^2}{E}C_{\text{int}}$$

$$\Psi_n = \tan^{-1}\left\{\frac{2\beta_n\Omega}{(\omega_n^2 - \Omega^2)}\right\}.\quad H_n = \int_0^L U_n(x)dx$$

$$\omega_n = K_n^2\sqrt{\frac{EI}{\rho a}},\quad \omega_{dn} = \omega_n\sqrt{1-\xi_n^2}$$

and

$$\beta_n = \xi_n\omega_n.$$

The constants, K_n, are the roots of

$$\cos(KL)\cosh(KL) = 1 \text{ for fixed ends}$$
$$\sin(KL)\sinh(KL) = 0 \text{ for simply supported ends.}$$

The beam functions are

$$U_n(x) = \cosh(K_n x) - \cos(K_n x) - \frac{\cos(K_n L) - \cosh(K_n L)}{\sin(K_n L) - \sinh(K_n L)}(\sinh(K_n x) - \sin(K_n x)) \text{ for fixed ends}$$

and

$$U_n(x) = \sin(K_n x) \text{ for simply supported ends.}$$

The orthogonality conditions

$$\int_0^L U_n(x)U_m(x) = 0 \text{ for } m \neq n$$
$$= C_1 \text{ for } m = n$$

allow determination of the constants, C_1, for the two end conditions. These are

$$C_1 = L \text{ for clamped boundaries}$$

and

$$C_1 = L/2 \text{ for simply supported ends.}$$

Displacement amplitudes are determined by making use of initial conditions with the result

$$A_n = F_n\sin\Psi_n$$

and

$$B_n = \frac{1}{\omega_{dn}}(\beta_n A_n - F_n\Omega\cos\Psi_n).$$

Equation (4) is valid for $0 \leq t \leq t_1$, where t_1 is the time of the first collision between the damper and the container (which is rig-

Nomenclature

a = cross-sectional area
A_0 = stress amplitude without the impact damper
A_d = stress amplitude with the impact damper
c_{ext} = coefficient of external damping
c_{int} = coefficient of internal damping
E = modulus of elasticity
h = amplitude of the base displacement
I = cross-sectional area moment of inertia
t = time coordinate
W = absolute transverse beam displacement
W_r = beam displacement relative to the support
x = distance along the beam
v = velocity of a particle
ξ = damping ratio
δ = Delta function
ρ = mass density
ω = natural frequency in radians per second
Ω = frequency of the base excitation
μ = ratio of the particle mass to the equivalent mass
$-,+$ = subscript designating quantities before and after the collision
$\cdot$ = derivative with respect to t
$[M]$ = diagonal mass matrix
$[K]$ = stiffness matrix
$[\Phi]$ = normalized modal matrix
$[\ ]^{-1}$ = inverse of a matrix
$[\ ]^T$ = transpose of a matrix
$\{\ \}$ = column matrix
$\lceil\ \rfloor$ = diagonal matrix

idly attached to the beam). The solution for subsequent periods between impacts is given by

$$W(x,t) = \sum_{n=1}^{\alpha} [\exp(-\beta_n t)\{A_{n+}\cos(\omega_{dn}t) + B_{n+}\sin(\omega_{dn}t)\} + F_n \sin(\Omega(t+t_1) - \Psi_n)]U_n(x) + h\sin\Omega(t+t_1) \quad (5)$$

Where t is reckoned from the time of collision and A_{n+}, B_{n+} are constants which are determined from the initial conditions just after each impact.

At the time of collision the beam displacement can be obtained either from equation (4) as $W_-(x,t_1)$ or from equation (5) as $W_+(x,0)$. By equating these two displacement expressions it is determined that

$$A_{n+} = \exp(-\beta_n t_1)\{A_n\cos(\omega_{dn}t_1) + B_n\sin(\omega_{dn}t_1)\}$$

For the collision it is assumed that the beam displacement remains constant while the velocity of the beam and the damper change discontinuously and that the damper particle experiences no friction drag when traveling with constant velocity before and after the impact. Further, if the beam is assumed to have an impact over the entire length with an impacting particle of mass m and velocity v, an incremental beam length must satisfy

$$\rho a\dot{W}_+(x,0)dx + v_+ m dx = \rho a\dot{W}_-(x,t_1)dx + v_- m dx$$

during the impact.

The conservation of momentum equation is obtained by integrating above equation over the entire beam length with impact restricted to occur only at a particular point, x_d. Thus the momentum equation becomes

$$\int_0^L \rho a\{\dot{W}_+(x,0) - \dot{W}_-(x,t_1)\}dx = \int_0^L (v_- - v_+)m\delta(x - x_d)dx. \quad (6)$$

Using equations (4), (5), and (6) there is obtained a relation involving the unknowns, B_{n+} and v_+, as

$$B_{n+} = (v - v_+)G_n + \frac{D_n}{\omega_{dn}} \quad (7)$$

where

$$G_n = \frac{mU_n(x_d)}{(\rho C_1 a\omega_{dn})}$$

and

$$D_n = A_{n+}\beta_n + \exp(-\beta_n t_1)\cos(\omega_{dn}t_1)(B_n\omega_{dn} + A_n\beta_n) + \exp(-\beta_n t_1)\sin(\omega_{dn}t_1)(A_n\omega_{dn} - B_n\beta_n).$$

By definition of the coefficient of restitution, e, between the particle and the beam

$$\dot{W}_+(x_d,0) - v_+ = -e(\dot{W}_-(x_d,t_1) - v_-)$$

which can be expressed as

$$v_+ = \sum_{n=1}^{\infty} U_n(x_d)\omega_{dn}B_{n+} + E_2. \quad (8)$$

In the latter equation

$$E_2 = \sum_{n=1}^{\infty} U_n(x_d)E_n + \Omega(1+e)h\cos\Omega t_1 - ev_-$$

where

$$E_n = e\{\exp(-\beta_n t_1)\cos(\omega_{dn}t_1)(B_n\omega_{dn} - A_n\beta_n) - \exp(-\beta_n t_1)\sin(\omega_{dn}t_1)(A_n\omega_{dn} + B_n\beta_n)\} - A_{n+}\beta_n + \Omega(1+e)F_n\cos(\Omega t_1 - \Psi_n).$$

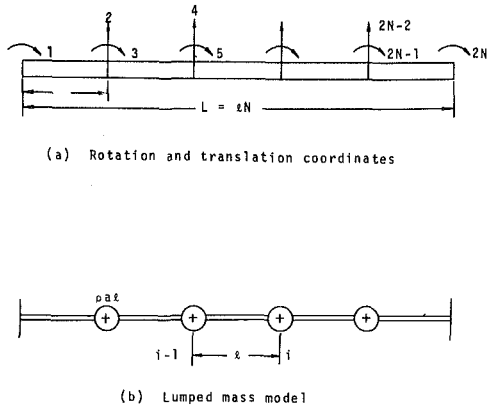

Fig. 3 Finite element model for fixed and simply supported beams

The solution of equation (7) and equation (8) for B_{n+} results in

$$B_{n+} + G_n\sum_{i=1}^{\infty} Z_i B_{i+} = R_n \quad (9)$$

where

$$Z_i = U_i(x_d)\omega_{di}$$

and

$$R_n = G_n v_- + \frac{D_n}{\omega_{dn}} - E_2 G_n.$$

Equation (9) represents a system of k nonhomogeneous equations in k unknowns (B_n, $n = 1, 2, 3, \ldots, k$), where only first k terms are utilized. The system of equations equation (9) can be solved to give solutions in the matrix form as

$$\begin{Bmatrix} B_{1+} \\ B_{2+} \\ \cdot \\ \cdot \\ B_{k+} \end{Bmatrix} = \begin{bmatrix} (1+G_1Z_1) & G_1Z_2 & \cdot\ \cdot & G_1Z_k \\ G_2Z_1 & (1+G_2Z_2) & \cdot\ \cdot & G_2Z_k \\ \cdot & \cdot & \cdot\ \cdot & \cdot \\ \cdot & \cdot & \cdot\ \cdot & \cdot \\ G_kZ_1 & \cdot & \cdot\ \cdot & (1+G_kZ_k) \end{bmatrix}^{-1} \begin{Bmatrix} R_1 \\ R_2 \\ \cdot \\ \cdot \\ R_k \end{Bmatrix}$$

The beam displacement between collisions is then given by equation (5) with A_{n+} and B_{n+} determined as discussed above.

The flexural stress at a point located on the surface of the beam is obtained by

$$\sigma = E\frac{\partial^2 W_r(x,t)}{\partial x^2}\cdot\frac{d}{2}$$

where d is the thickness of the beam.

2 Finite Element Solution

The governing differential equation of motion for a lumped mass model of a Bernoulli-Euler beam, as shown in Fig. 3, can be represented as

$$\left[\begin{array}{c|c} M & 0 \\ \hline 0 & J \end{array}\right]\begin{Bmatrix} \ddot{Y} \\ \ddot{\theta} \end{Bmatrix} + \left[\begin{array}{c|c} K_{11} & K_{12} \\ \hline K_{21} & K_{22} \end{array}\right]\begin{Bmatrix} Y \\ \theta \end{Bmatrix} = \begin{Bmatrix} 0 \\ \hline 0 \end{Bmatrix}$$

Neglecting $J_i\ddot{\theta}_i(\ll M_i\ddot{Y})$ for lower modes and with base excitation, the equation of motion in displacement coordinates can be expressed as

$$[M]\{\ddot{Y}_r\} + [C]\{\dot{Y}_r\} + [S]\{Y_r\} = \{M_i\}h\Omega^2\sin\Omega t \quad (10)$$

where

$$\{Y_r\} = \{Y\} - \{1\}h\sin\Omega t \quad (10a)$$

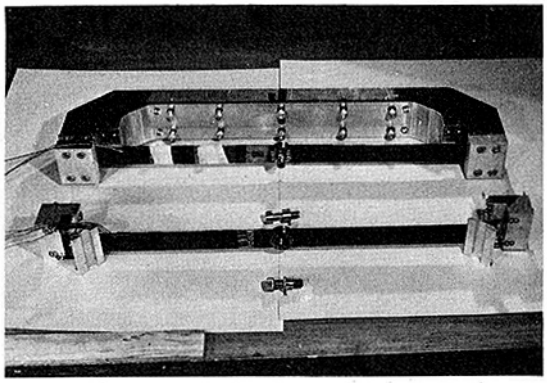

Fig. 4 Photograph of the beams and support fixture

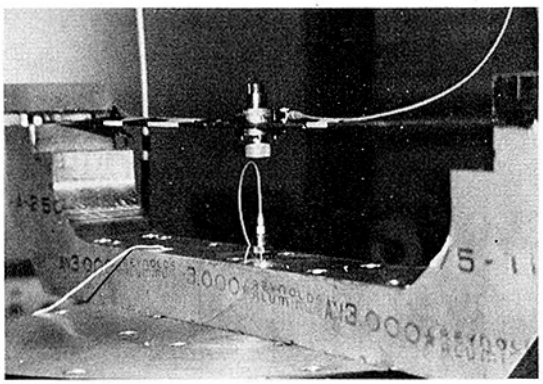

Fig. 6 A photograph of the assembled fixture-beam-damper unit

$$[S] = [K_{11}] - [K_{12}][K_{22}]^{-1}[K_{21}],$$
$$\{\theta\} = -[K_{22}]^{-1}[K_{21}]\{Y\} \tag{10b}$$

and $[C]$ is a diagonal damping matrix obtained by a linear combination of mass and stiffness matrices.

Following the standard approach used in the theory of differential equations, the complete solution of equation (10) can be cast in the form

$$\{Y\} = [\Phi]\left[\exp(-\xi_i\omega_i t)\right]\left\{\left[\sin\omega_{di}t\right]\{A_i\} + \left[\cos\omega_{di}t\right]\{B_i\}\right\} + \frac{[\Phi]}{\bar{m}}\left[\frac{(P_i\sin\Omega t - Q_i\cos\Omega t)}{P_i^2 + Q_i^2}\right]\{F\} + \{1\}h\sin\Omega t \tag{11}$$

where

$$\omega_{di} = \omega_i\sqrt{1-\xi_i^2}$$
$$P_i = \omega_i^2 - \Omega^2$$
$$Q_i = 2\xi_i\omega_i\Omega$$

and

$$\bar{m} = [\Phi]^T[M][\Phi]$$

The array, $[\Phi]$, is the normalized modal matrix and $\{A_i\}$ and $\{B_i\}$ are constants determined by the initial conditions.

If the impact damper is located at any of the node points and a collision between the beam and the particle occurs at time $t = t_1$, then the solution after the impact can be established as

$$\{Y\} = [\Phi]\left[\exp(-\xi_i\omega_i t)\right]\left\{\left[\sin\omega_{di}t\right]\{A_{i+}\} + \left[\cos\omega_{di}t\right]\{B_{i+}\}\right\} + \frac{[\Phi]}{\bar{m}}\left[\frac{P_i\sin\Omega(t+t_1) + Q_i\cos\Omega(t+t_1)}{P_i^2 + Q_i^2}\right]\{F\} + \{1\}h\sin\Omega(t+t_1) \tag{11a}$$

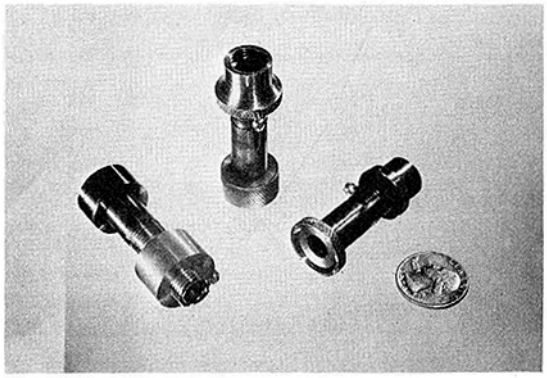

Fig. 5 Photograph of the damper units used in the experimental phase

where t is time elapsed after the impact and A_{i+} and B_{i+} are constants which are evaluated by using the initial conditions just after the impact.

Since the displacements remain unchanged during the impact, equating equation (11) and equation (11a) at the time of collision gives

$$B_{i+} = \exp(-\omega_i\xi_i t_i)(A_i\sin\omega_{di}t_1 + B_i\cos\omega_{di}t_1). \tag{12}$$

The motion of the damper particle of mass m, and the mass at the damper location including the container mass, must satisfy the momentum equation during the impact. Therefore,

$$m_d\dot{Y}_{d-} + mv_- = m_d\dot{Y}_{d+} + mv_+ \tag{13}$$

where $\dot{Y}_{d-}$, v_- and $\dot{Y}_{d+}$, v_+ are the system velocities before and after the impact, respectively.

Again using e as the coefficient of restitution between the impacting materials, momentum consideration gives

$$\dot{Y}_{d+} - v_+ = -e(\dot{Y}_{d-} - v_-). \tag{14}$$

Equation (13) and equation (14) can be solved to give

$$v_+ = \frac{\{\dot{Y}_{d-} + v_-m/m_d + e(\dot{Y}_{d-} - v_-)\}}{(1 + m/m_d)}$$

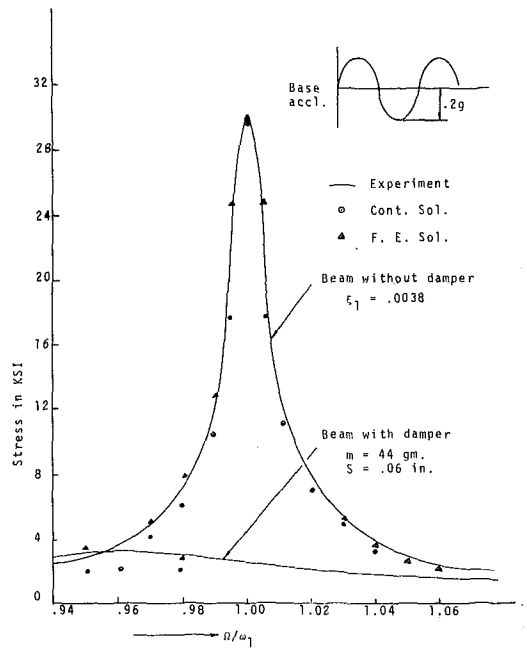

Fig. 7 First mode frequency response of the simply supported beam

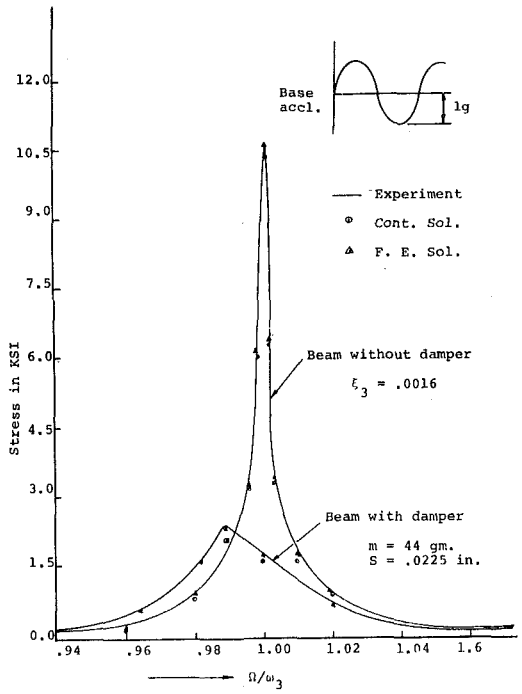

Fig. 8 Third mode frequency response of the simply supported beam

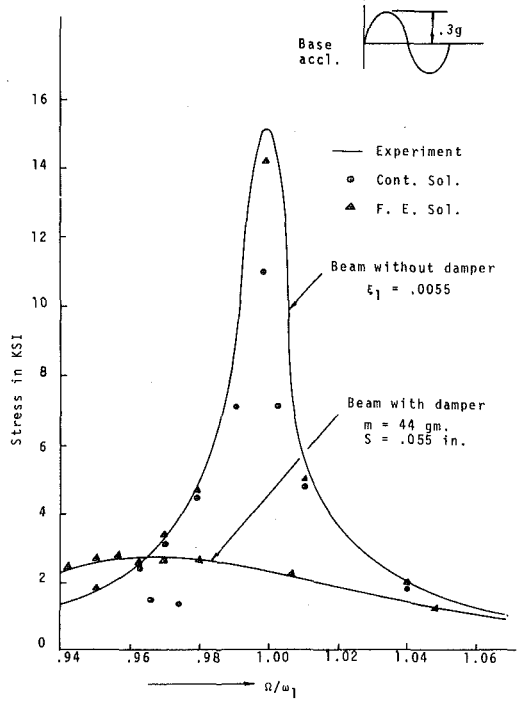

Fig. 9 First mode frequency response of the fixed beam

and

$$\dot{Y}_{d+} = \frac{\{\dot{Y}_{d-} + v_-m/m_d + e(\dot{Y}_{d-} - v_-)\}}{(1 + m/m_d)} - e(\dot{Y}_d - v_-).$$

Velocities of all the lumped masses except the one where damper is located, are the same before and after the collision and are obtained by differentiating equation (11) with respect to time at $t = t_1$. Velocities of the lumped masses just after the impact thus become

$$\{\dot{Y}_{i+}\} = \begin{Bmatrix} \dot{Y}_{1-} \\ \dot{Y}_{2-} \\ \dot{Y}_{d+} \\ \dot{Y}_{i-} \end{Bmatrix} \tag{15}$$

Since the solution given by equation (11a) must satisfy the initial conditions as specified by equation (15) for velocities, the constants, A_{i+}, are obtained as follows

$$\{A_{i+}\} = [\omega_{di}]^{-1}\{\omega_i \xi_i B_{i+}\} - \frac{1}{m}[\Phi]^T[M]\{h\Omega \cos \Omega t_1 - Y_{i+}\} - \frac{1}{m}[\omega_{di}]\left[\frac{(P_i \cos \Omega t_1 + Q_i \sin \Omega t_1)}{P_i^2 + Q_i^2}\right]\{F\}. \tag{16}$$

The complete solution for the displacement of the beam after the collision is obtained by evaluating equation (11a) with the new values of A_{i+} and B_{i+} determined from equation (16) and equation (12), respectively. The corresponding rotation at each node at the same time is computed by using equation (10b).

Forces and moments acting on an element can be determined from the relation

$$\begin{Bmatrix} f_i \\ f_{i+1} \\ M_i \\ M_{i+1} \end{Bmatrix} = \frac{2EI}{l^3}\begin{bmatrix} 6 & -6 & -3l & -3l \\ -6 & 6 & 3l & 3l \\ -3l & 3l & 2l^2 & l^2 \\ -3l & 3l & l^2 & 2l^2 \end{bmatrix}\begin{Bmatrix} Y_i \\ Y_{i+1} \\ \theta_i \\ \theta_{i+1} \end{Bmatrix}$$

Thus the bending stress on the surface of the beam at the ith node is

$$\sigma_i = \frac{M_i}{I} \cdot \frac{d}{2}$$

3 Numerical Computation

In the previous two sections solutions have been derived which are valid during the time between collisions. In so doing, the time t_1 at which the first impact occurs is assumed to be known. The times of all impacts are actually determined by numerical computation of the equations established.

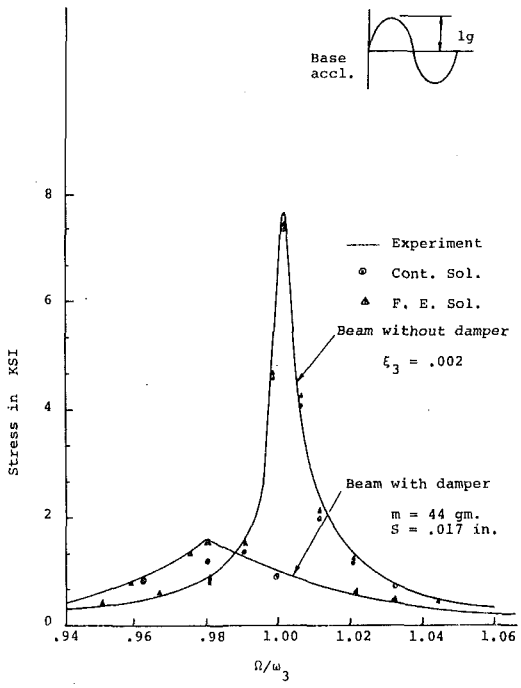

Fig. 10 Third mode frequency response of the fixed beam

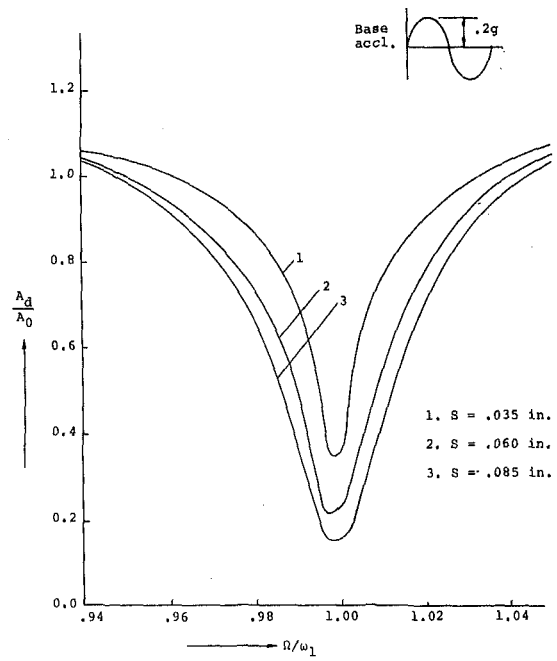

Fig. 11 First mode isolation curves for the simply supported beam (17 g damper)

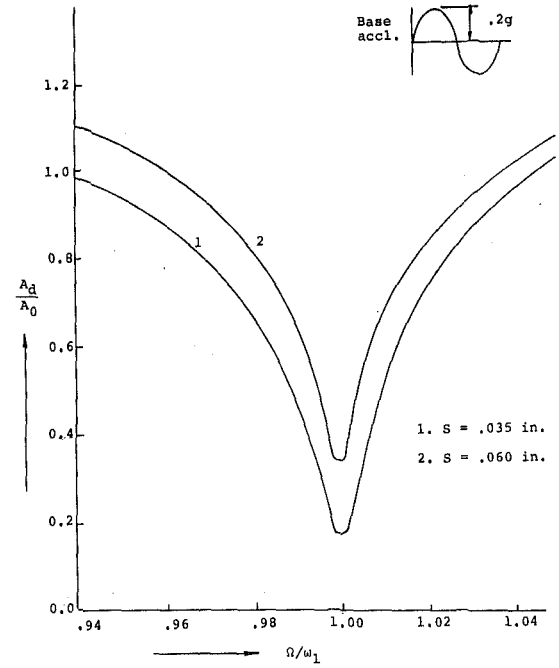

Fig. 13 First mode isolation curves for the simply supported beam (73 g damper)

If the beam displacement at the damper location is denoted by $U_d(t)$, then

$U_d(t)$ = either the solution equation (5) evaluated at $x = x_d$ or one of the solutions equation (11a) for the lumped mass with the damper mass.

The particle displacement, $U_p(t)$, is measured from the initial reference position of the damper on the beam. Then, in order that the particle might come in contact with either of the container ends, $U_d(t)$ and $U_p(t)$ must satisfy

$$|U_d(t) - U_p(t)| = S/2$$

where S is the clearance.

A measure of how close the system is to an impact is indicated by the difference of the quantities appearing on the left and the right hand sides of the above equation. Therefore, the roots of

$$S/2 - |U_d(t) - U_p(t)| = 0$$

are the times of collisions and were determined by a standard iteration technique.

All computation were carried out with the coefficient of restitution between the damper and the beam, $e = 0.8$.

4 Experimental Investigation

The two solutions, continuous beam and discrete mass system, were used together with experimental tests to complete the inves-

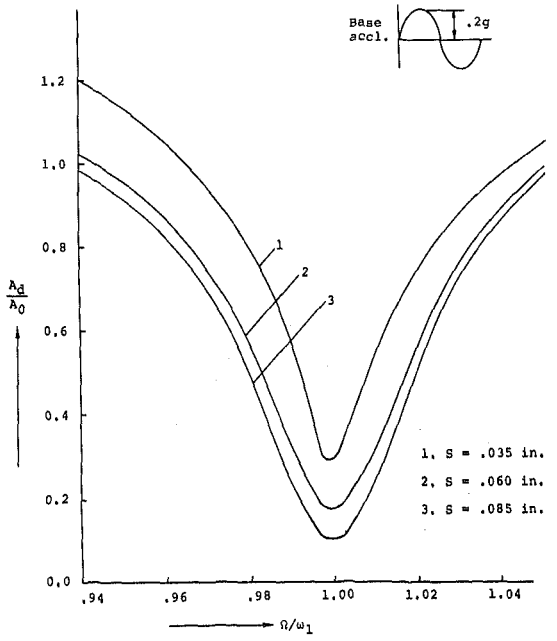

Fig. 12 First mode isolation curves for the simply supported beam (44 g damper)

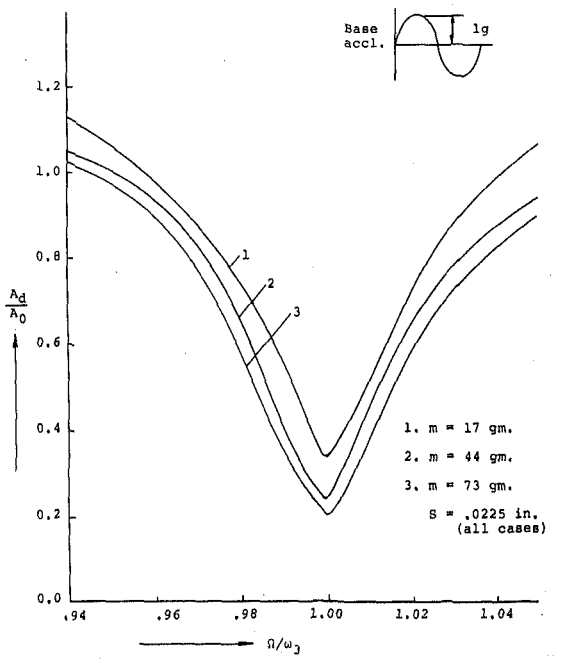

Fig. 14 Third mode isolation curves for the simply supported beam

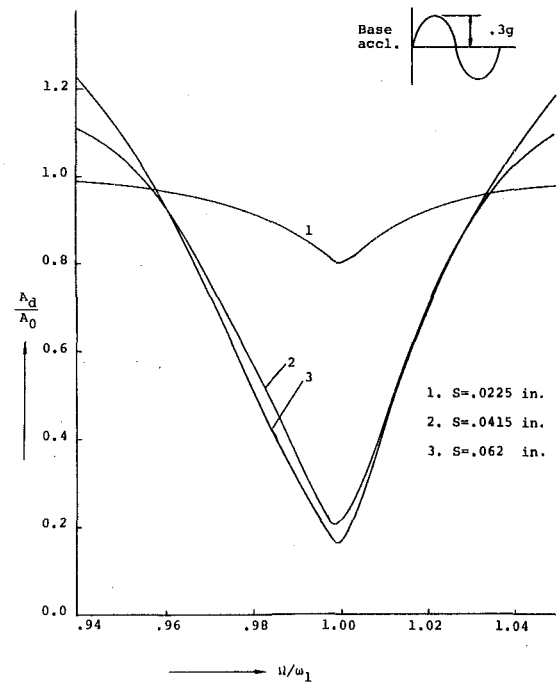

Fig. 15 First mode isolation curves for the fixed beam (17 g damper)

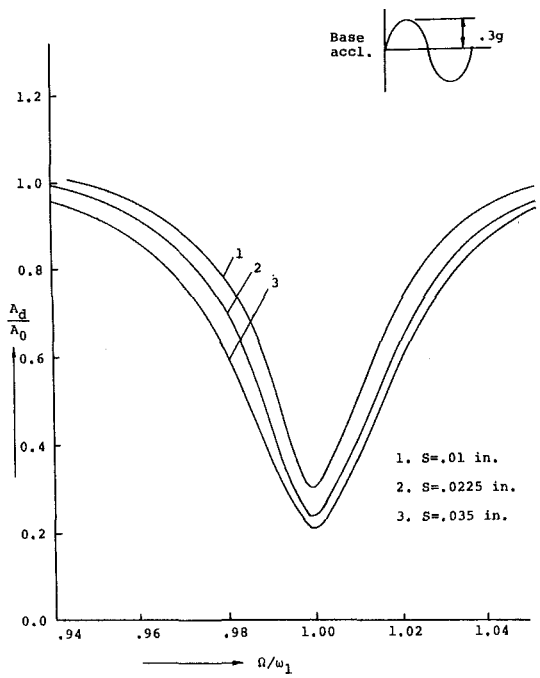

Fig. 17 First mode isolation curves for the fixed beam (73 g damper)

tigation. The finite element procedure was checked against the continuous system solution to insure sufficient numbers of discrete masses were included. This system was further compared with experimental results to obtain damping coefficients.

The experimental phase was necessary to obtain information concerning the design and use of impact dampers applied to continuous systems. Tests were conducted on two types of steel beams. The beams were machined from ⅛ in. thick steel plate and were 1½ in. wide by 25½ in. long. Support fixtures were designed to permit positioning of these beams as either clamped or simply supported for the two different tests. A photograph of the beams and support fixture is shown in Fig. 4. The entire experimental work was conducted on a 3500 lb-force MB C25H vibration exciter.

The damper unit consisted of a pair of hard steel collars attached to the beam and an alloy steel nut and bolt assembly. A photograph of the damper unit is shown in Fig. 5. The bolt was fitted into a hole drilled through the beam and was constrained to oscillate within a certain magnitude of clearance which was varied for each test. The impact damper in both models was located at the center of each beam. A photograph of the mounted unit is shown in Fig. 6.

Strain and acceleration of both types of beams were recorded at $x = 11.165$ in. and $x = 14.36$ in., respectively, along the length. The strain amplitude was utilized for purposes of comparison. All values were well within the elastic range.

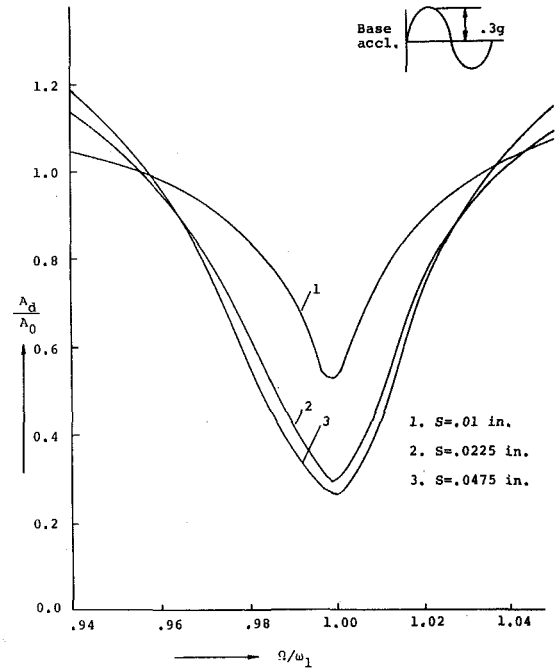

Fig. 16 First mode isolation curves for the fixed beam (44 g damper)

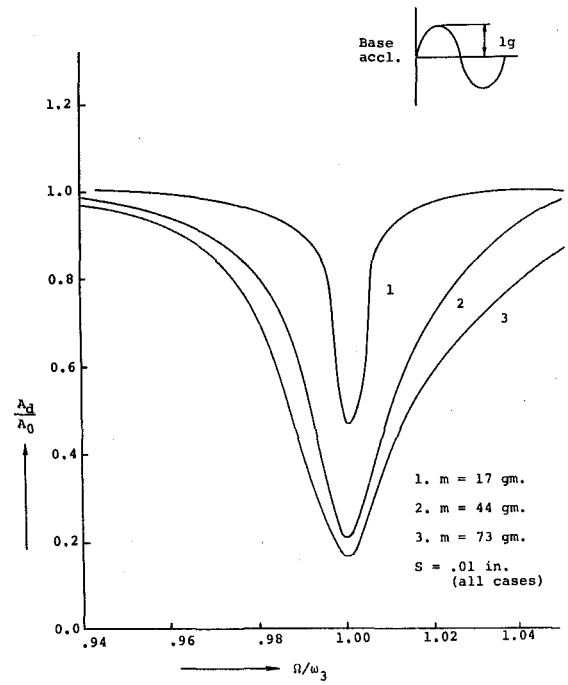

Fig. 18 Third mode isolation curves for the fixed beam

5 Discussion of Results

Computer solutions were carried out using ten terms for the continuous system calculation and with eight segments in the finite element analysis. The results of these computations are compared with experimental findings in Figs. 7 and 8 for the simply supported beam and Figs. 9 and 10 for the fixed beam. The effectiveness of the impact damper in reducing the stress is readily observed.

Figs. 11 thru 18 show the results of an experimental parameter study which would be useful in applying impact dampers to these types of systems. In the figures the ordinate, A_d/A_0, is the ratio of the maximum amplitude of the system with an attached damper to that of the same system without a damper and is termed as isolation factor. Again the effectiveness is easily seen for a range of parametric values.

The amplitude response was observed to reduce to a minimum for a particular clearance and increase from the low as the clearance was gradually increased. A heavier damper particle was more effective in reducing response in the primary mode. The effectiveness measured as amplitude reduction was seen to be dependent on the base excitation.

Although it has not been included in the paper, experimental results from this work also compares favorably with the reported data of Masri and Caughey [3]. To make the comparison the continuous systems used herein were reduced to an equivalent single degree-of-freedom system based on the first mode response. Good correlation was obtained with this analysis.

6 Conclusions

A seminumerical technique has been developed to describe the motion of sinusoidally excited, continuous systems with attached impact dampers. The two systems consisted of a simply supported and a clamped beam. Experimental verification of results was obtained by using the two types of beams and three different dampers.

As a result of the study it has been found that:

(a) The impact damper is very effective in reducing vibration amplitudes near the resonant frequencies.

(b) The performance of the damper was observed to be dependent on the magnitude of the base excitation attesting to the nonlinear character of this device.

(c) Heavier damper particles produce more isolation near a resonance.

(d) For a damper of given mass, a particular clearance produced the most effective reduction in response.

(e) Very good agreement was obtained between analytical and experimental results.

References

1 Grubin, C., "On the Theory of the Acceleration Damper," *Journal of Applied Mechanics,* TRANS. ASME, Sept. 1956, pp. 373–378.

2 Arnold, R. N., "Response of an Impact Vibration Absorber to Forced Vibration," Ninth International Congress of Applied Mechanics, 1956.

3 Masri, S. F., and Caughey, T. K., "On the Stability of the Impact Damper," *Journal of Applied Mechanics,* TRANS. ASME, Sept. 1966, pp. 586–592.

4 Masri, S. F., "Steady-State Response of a Multi-Degree System with an Impact Damper," *The Journal of the Acoustical Society of America,* Vol. 45, No. 5, 1969.

5 Masri, S. F., "Forced Vibration of Glass of Nonlinear Dissipative Beams," *Journal of the Engineering Mechanics Division,* ASCE Vol. 99, No. EM4, Proc. Paper 9959, August 1973, pp. 669–683.

6 Masri, S. F., and Kahyai, K., "Steady-State Motion of a Plate with a Discontinuous Mass," *Int. J. Non-Linear Mechanics,* Pergamon Press, Vol. 9, 1974, pp. 451–462.